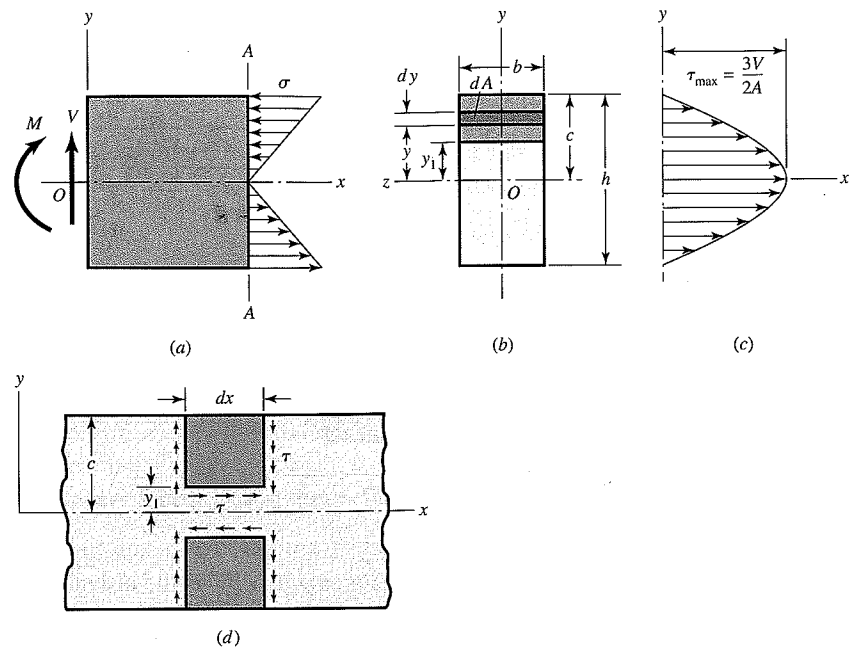**Figure 3-18**

Transverse shear stresses in a rectangular beam.

(a)   (b)   (c)

(d)

If we now use this value of I for Eq. (3-32) and rearrange, we get

$$\tau = \frac{3V}{2A}\left(1 - \frac{y_1^2}{c^2}\right) \tag{3-33}$$

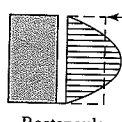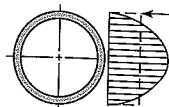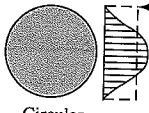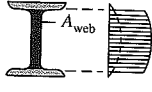We note that the maximum shear stress exists when $y_1 = 0$, which is at the bending neutral axis. Thus

$$\tau_{max} = \frac{3V}{2A} \tag{3-34}$$

for a rectangular section. As we move away from the neutral axis, the shear stress decreases parabolically until it is zero at the outer surfaces where $y_1 = \pm c$, as shown in Fig. 3-18c. Horizontal shear stress is always accompanied by vertical shear stress of the same magnitude, and so the distribution can be diagrammed as shown in Fig. 3-18d. Figure 3-18c shows that the shear τ on the vertical surfaces varies with y. We are almost always interested in the horizontal shear, τ in Fig. 3-18d, which is nearly uniform over dx with constant $y = y_1$. The maximum horizontal shear occurs where the vertical shear is largest. This is usually at the neutral axis but may not be if the width b is smaller somewhere else. Furthermore, if the section is such that b can be minimized on a plane not horizontal, then the horizontal shear stress occurs on an inclined plane. For example, with tubing, the horizontal shear stress occurs on a radial plane and the corresponding "vertical shear" is not vertical, but tangential.

The distributions of transverse shear stresses for several commonly used cross sections are shown in Table 3-2. The profiles represent the VQ/Ib relationship, which is a function of the distance y from the neutral axis. For each profile, the formula for the maximum value at the neutral axis is given. Note that the expression given for the I beam is a commonly used approximation that is reasonable for a standard I beam with a thin web. Also, the profile for the I beam is idealized. In reality the transition from the web to the flange is quite complex locally, and not simply a step change.

Table 3–2

Formulas for Maximum
Transverse Shear Stress
from VQ/Ib

Beam Shape	Formula	Beam Shape	Formula
Rectangular $\quad \tau_{avc} = \dfrac{V}{A}$	$\tau_{max} = \dfrac{3V}{2A}$	Hollow, thin-walled round $\quad \tau_{avc} = \dfrac{V}{A}$	$\tau_{max} = \dfrac{2V}{A}$
Circular $\quad \tau_{avc} = \dfrac{V}{A}$	$\tau_{max} = \dfrac{4V}{3A}$	Structural I beam (thin-walled) $\quad A_{web}$	$\tau_{max} \doteq \dfrac{V}{A_{web}}$

It is significant to observe that the transverse shear stress in each of these common cross sections is maximum on the neutral axis, and zero on the outer surfaces. Since this is exactly the opposite of where the bending and torsional stresses have their maximum and minimum values, the transverse shear stress is often not critical from a design perspective.

Let us examine the significance of the transverse shear stress, using as an example a cantilever beam of length L, with rectangular cross section $b \times h$, loaded at the free end with a transverse force F. At the wall, where the bending moment is the largest, at a distance y from the neutral axis, a stress element will include both bending stress and transverse shear stress. In Sec. 5–4 it will be shown that a good measure of the combined effects of multiple stresses on a stress element is the maximum shear stress. Inserting the bending stress (My/I) and the transverse shear stress (VQ/Ib) into the maximum shear stress equation, Eq. (3–14), we obtain a general equation for the maximum shear stress in a cantilever beam with a rectangular cross section. This equation can then be normalized with respect to L/h and y/c, where c is the distance from the neutral axis to the outer surface ($h/2$), to give

$$\tau_{max} = \sqrt{\left(\frac{\sigma}{2}\right)^2 + \tau^2} = \frac{3F}{2bh}\sqrt{4(L/h)^2(y/c)^2 + \left[1 - (y/c)^2\right]^2} \qquad (d)$$

To investigate the significance of transverse shear stress, we plot τ_{max} as a function of L/h for several values of y/c, as shown in Fig. 3–19. Since F and b appear only as linear multipliers outside the radical, they will only serve to scale the plot in the vertical direction without changing any of the relationships. Notice that at the neutral axis where $y/c = 0$, τ_{max} is constant for any length beam, since the bending stress is zero at the neutral axis and the transverse shear stress is independent of L. On the other hand, on the outer surface where $y/c = 1$, τ_{max} increases linearly with L/h because of the bending moment. For y/c between zero and one, τ_{max} is nonlinear for low values of L/h, but behaves linearly as L/h increases, displaying the dominance of the bending stress as the moment arm increases. We can see from the graph that the critical stress element (the largest value of τ_{max}) will always be either on the outer surface ($y/c = 1$) or at the neutral axis ($y/c = 0$), and never between. Thus, for the rectangular cross section, the transition between these two locations occurs at $L/h = 0.5$ where the line for $y/c = 1$ crosses the horizontal line for $y/c = 0$. The critical stress element is either on the outer

3–12 **Torsion**

Any moment vector that is collinear with an axis of a mechanical element is called a
torque vector, because the moment causes the element to be twisted about that axis. A
bar subjected to such a moment is also said to be in *torsion.*

As shown in Fig. 3–21, the torque T applied to a bar can be designated by drawing
arrows on the surface of the bar to indicate direction or by drawing torque-vector arrows
along the axes of twist of the bar. Torque vectors are the hollow arrows shown on the
x axis in Fig. 3–21. Note that they conform to the right-hand rule for vectors.

The *angle of twist,* in radians, for a solid round bar is

$$\theta = \frac{Tl}{GJ} \tag{3–35}$$

where T = torque

l = length

G = modulus of rigidity

J = polar second moment of area

Shear stresses develop throughout the cross section. For a round bar in torsion,
these stresses are proportional to the radius ρ and are given by

$$\tau = \frac{T\rho}{J} \tag{3–36}$$

Designating r as the radius to the outer surface, we have

$$\tau_{\max} = \frac{Tr}{J} \tag{3–37}$$

The assumptions used in the analysis are:

- The bar is acted upon by a pure torque, and the sections under consideration are
  remote from the point of application of the load and from a change in diameter.
- The material obeys Hooke's law.
- Adjacent cross sections originally plane and parallel remain plane and parallel after
  twisting, and any radial line remains straight.

I Figure 3–21
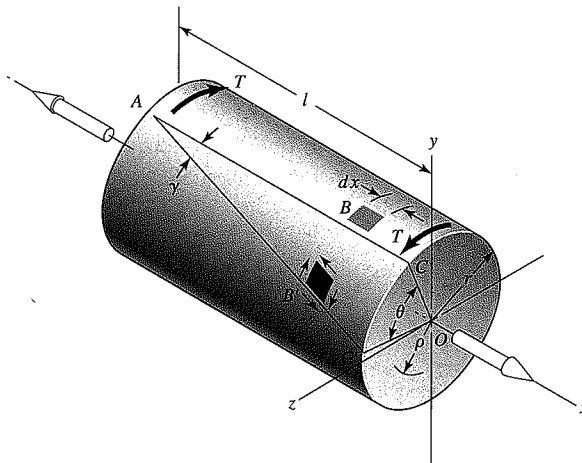
A *theoretical,* or *geometric, stress-concentration factor* K_t or K_{ts} is used to relate the actual maximum stress at the discontinuity to the *nominal stress.* The factors are defined by the equations

$$K_t = \frac{\sigma_{max}}{\sigma_0} \qquad K_{ts} = \frac{\tau_{max}}{\tau_0} \qquad (3\text{--}48)$$

where K_t is used for normal stresses and K_{ts} for shear stresses. The nominal stress σ_0 or τ_0 is the stress calculated by using the elementary stress equations and the net area, or net cross section. Sometimes the gross cross section is used instead, and so it is always wise to double check the source of K_t or K_{ts} before calculating the maximum stress.

The stress-concentration factor depends for its value only on the *geometry* of the part. That is, the particular material used has no effect on the value of K_t. This is why it is called a *theoretical* stress-concentration factor.

The analysis of geometric shapes to determine stress-concentration factors is a difficult problem, and not many solutions can be found. Most stress-concentration factors are found by using experimental techniques.[9] Though the finite-element method has been used, the fact that the elements are indeed finite prevents finding the true maximum stress. Experimental approaches generally used include photoelasticity, grid methods, brittle-coating methods, and electrical strain-gauge methods. Of course, the grid and strain-gauge methods both suffer from the same drawback as the finite-element method.

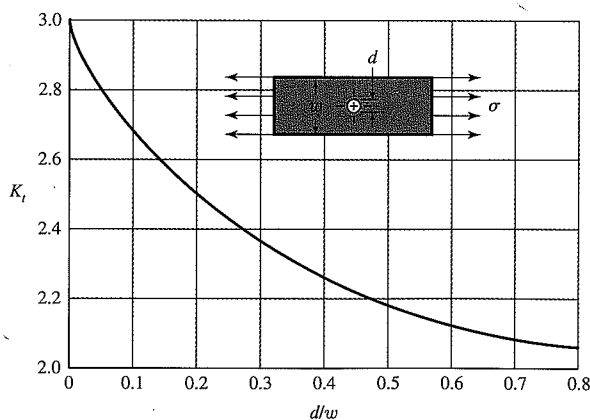Stress-concentration factors for a variety of geometries may be found in Tables A–15 and A–16.

An example is shown in Fig. 3–29, that of a thin plate loaded in tension where the plate contains a centrally located hole.

In *static loading,* stress-concentration factors are applied as follows. In *ductile materials* ($\epsilon_f \geq 0.05$), the stress-concentration factor *is not* usually applied to predict the critical stress, because plastic strain in the region of the stress is localized and has a strengthening effect. In *brittle materials* ($\epsilon_f < 0.05$), the geometric stress-concentration factor K_t is applied to the nominal stress before comparing it with strength. Gray cast iron has so many inherent stress raisers that the stress raisers introduced by the designer have only a modest (but additive) effect.

Figure 3-29

Thin plate in tension or simple compression with a transverse central hole. The net tensile force is $F = \sigma wt$, where t is the thickness of the plate. The nominal stress is given by

$$\sigma_0 = \frac{F}{(w-d)t} = \frac{w}{(w-d)}\sigma$$

[9]The best source book is W. D. Pilkey and D. F. Pilkey, *Peterson's Stress Concentration Factors,* 3rd ed., John Wiley & Sons, New York, 2008.

Table A–18

Geometric Properties

Part 1 Properties of Sections

A = area

G = location of centroid

$$I_x = \int y^2 \, dA = \text{second moment of area about } x \text{ axis}$$

$$I_y = \int x^2 \, dA = \text{second moment of area about } y \text{ axis}$$
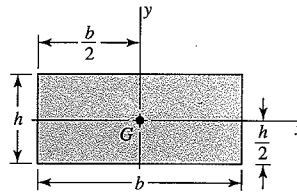
$$I_{xy} = \int xy \, dA = \text{mixed moment of area about } x \text{ and } y \text{ axes}$$

$$J_G = \int r^2 \, dA = \int (x^2 + y^2) \, dA = I_x + I_y$$
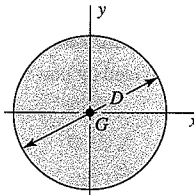
= second polar moment of area about axis through G

$k_x^2 = I_x / A$ = squared radius of gyration about x axis

Rectangle

$$A = bh \qquad I_x = \frac{bh^3}{12} \qquad I_y = \frac{b^3 h}{12} \qquad I_{xy} = 0$$

Circle

$$A = \frac{\pi D^2}{4} \qquad I_x = I_y = \frac{\pi D^4}{64} \qquad I_{xy} = 0 \qquad J_G = \frac{\pi D^4}{32}$$

Hollow circle
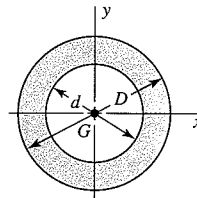
$$A = \frac{\pi}{4}(D^2 - d^2) \qquad I_x = I_y = \frac{\pi}{64}(D^4 - d^4) \qquad I_{xy} = 0 \qquad J_G = \frac{\pi}{32}(D^4 - d^4)$$
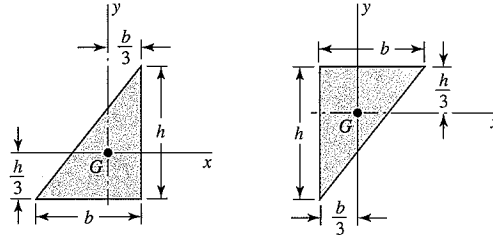
Table A–18

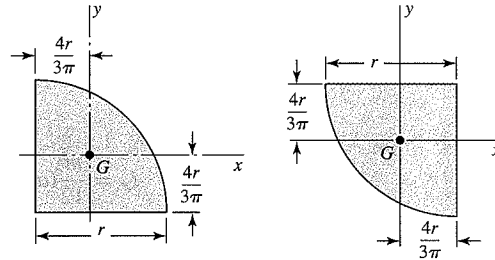Geometric Properties
(Continued)

Right triangles
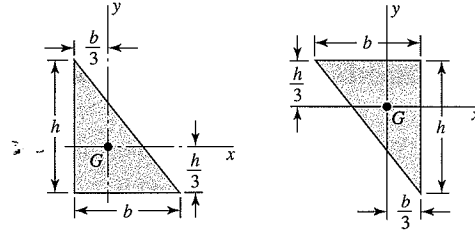
$$A = \frac{bh}{2} \qquad I_x = \frac{bh^3}{36} \qquad I_y = \frac{b^3h}{36} \qquad I_{xy} = \frac{-b^2h^2}{72}$$
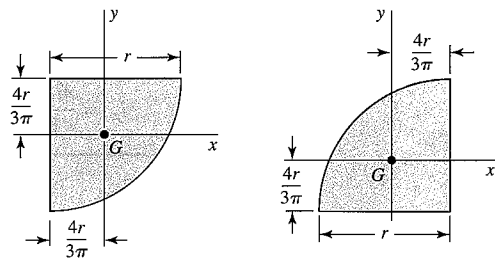
Right triangles

$$A = \frac{bh}{2} \qquad I_x = \frac{bh^3}{36} \qquad I_y = \frac{b^3h}{36} \qquad I_{xy} = \frac{b^2h^2}{72}$$

Quarter-circles

$$A = \frac{\pi r^2}{4} \qquad I_x = I_y = r^4\left(\frac{\pi}{16} - \frac{4}{9\pi}\right) \qquad I_{xy} = r^4\left(\frac{1}{8} - \frac{4}{9\pi}\right)$$

Quarter-circles

$$A = \frac{\pi r^2}{4} \qquad I_x = I_y = r^4\left(\frac{\pi}{16} - \frac{4}{9\pi}\right) \qquad I_{xy} = r^4\left(\frac{4}{9\pi} - \frac{1}{8}\right)$$
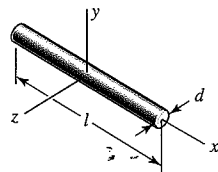
(continued)
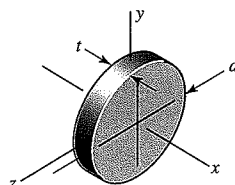
Table A–18

Geometric Properties
(Continued)

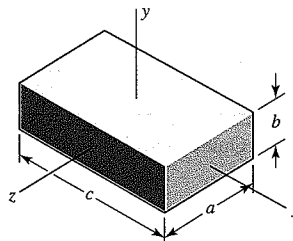**Part 2 Properties of Solids (ρ = Density, Weight per Unit Volume)**

Rods

$$m = \frac{\pi d^2 l \rho}{4g} \qquad I_y = I_z = \frac{ml^2}{12}$$
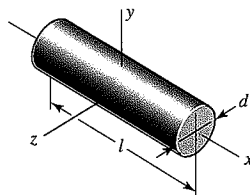
Round disks

$$m = \frac{\pi d^2 t \rho}{4g} \qquad I_x = \frac{md^2}{8} \qquad I_y = I_z = \frac{md^2}{16}$$
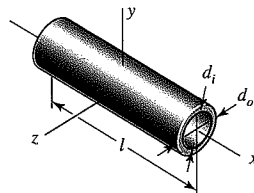
Rectangular prisms

$$m = \frac{abc\rho}{g} \qquad I_x = \frac{m}{12}(a^2 + b^2) \qquad I_y = \frac{m}{12}(a^2 + c^2) \qquad I_z = \frac{m}{12}(b^2 + c^2)$$

Cylinders

$$m = \frac{\pi d^2 l \rho}{4g} \qquad I_x = \frac{md^2}{8} \qquad I_y = I_z = \frac{m}{48}(3d^2 + 4l^2)$$

Hollow cylinders

$$m = \frac{\pi \left(d_o^2 - d_i^2\right) l \rho}{4g} \qquad I_x = \frac{m}{8}\left(d_o^2 + d_i^2\right) \qquad I_y = I_z = \frac{m}{48}\left(3d_o^2 + 3d_i^2 + 4l^2\right)$$